Journal of Food Engineering 200 (2017) 70–80

Contents lists available at ScienceDirect

Journal of Food Engineering

journal homepage: www.elsevier.com/locate/jfoodeng

Cold sterilization and process modeling of tender coconut water by hollow fibers

Sankha Karmakar, Sirshendu De*

Department of Chemical Engineering, Indian Institute of Technology Kharagpur, Kharagpur, 721302, India

ARTICLE INFO

Article history:
Received 5 March 2016
Received in revised form
18 August 2016
Accepted 29 December 2016
Available online 2 January 2017

Keywords:
Cold sterilization
Tender coconut water
Resistance-in-series model
Storage study

ABSTRACT

Tender coconut water is one of the popular sport drinks. In this paper, cold sterilization of tender coconut water was undertaken using hollow fiber ultrafiltration. Experiments were conducted at different transmembrane pressures in the range of 21–193 kPa and cross flow rate 5–15 l/h to optimize the operating conditions. A simple resistance-in-series model was used to quantify the flux decline behavior. A mathematical criterion between the operating conditions was derived for limiting flux. This is of immense importance for process modeling, scaling up and control of operating conditions of such systems. Various parameters of the feed and permeate, namely, total soluble solids, pH, clarity, concentration of sodium, potassium, polyphenol, protein and total solids were monitored. A subsequent storage study was undertaken and it was observed that the filtered juice was successfully stored for 18 weeks. This study was adequately backed up by conducting a taste analysis.

1. Introduction

Fruit juices are rich in minerals, proteins, anti-oxidants and have potential for rejuvenating the body and therefore, have a huge demand in today's world (Sagu et al., 2014). Coconut water is a natural beverage with high nutritional value and is considered as energy drink to joggers and athletes. Thus, to reduce the transportation volume and cost associated with the whole fruit and to improve the shelf life of tender coconut water, its processing is necessary. Tender coconut water is rich in essential minerals, like, potassium, sodium and natural nutrients, like, polyphenol (Yong et al., 2009). It is a good sports drink and has therapeutic values (Saat et al., 2002). It is available plenty in coastal areas and hence, it has a high demand in the areas interior to the country where coconut is not available. It is a good export item as well. The fresh coconut water has a shelf life of about 24 h (Reddy et al., 2005) and that can be enhanced by ultra-high temperature, pasteurization, refrigeration, freezing and microwave heating (Matsui et al., 2007).

Due to presence of sugar and a number of plant enzymes (Jackson et al., 2004), the tender coconut water has a strong tendency to undergo biochemical changes and spoilage, once the nuts are harvested from the tree. Efforts are made to arrest these changes by packing the nuts in plastic films and storing them at refrigeration temperature (Maciel et al., 1992). The above method is expensive in terms of energy and transportation cost and has lower shelf life of 2–3 weeks. The coconut water is processed by high temperature short time pasteurization in Thailand, Indonesia and Philippines (Magda, 1992). Polyphenol oxidase and peroxidise are the major plant enzymes causing the spoilage and loss of nutritional qualities of tender coconut water. Campos et al. (1996) studied the inactivation of these enzymes by heat treatment at 90 °C for 100 s with additives like ascorbic acid and potassium meta-bisulphite. Addition of these external chemicals deteriorates the taste and quality parameters of the treated juice significantly. Thermal processing is usually carried out between 60°C and 100 °C and it eliminates not only bacteria but also the entire delicate flavour profile is almost hampered. This severely limits the marketability of the product. Matsui et al. (2008) studied inactivation kinetics of these enzymes by microwave heating in tender coconut water. The process was carried at 90 °C, degrading the sensory properties of the juice. Membrane based processes offer attractive alternative in this regard.

Literature on membrane filtration of tender coconut water is scant. Magalhaes et al. (2005), reported filtration by 0.1 μm microfiltration (MF) and three cut off (20, 50 and 100 kDa) ultrafiltration (UF) membranes. Significant reduction in turbidity, microorganism and 24%–40% reduction in protein was obtained. The filtration was associated with severe (87%–93%) flux decline.

* Corresponding author.
E-mail address: sde@che.iitkgp.ernet.in (S. De).

http://dx.doi.org/10.1016/j.jfoodeng.2016.12.021
0260-8774/

However, a systematic storage study was not attempted with an appropriate selection of membrane. Reddy et al. (2007) used a two stage filtration process by whatman filter paper followed by 0.2 μm MF membrane. The final permeate was stored for one month only and its acceptability was reduced due to significant loss in sugar and other nutritional parameters. They also reported the development of significant fouling resistance over the membrane surface (Reddy et al., 2005). However, this study was purely in laboratory scale and had marginal significance in scaling up. Jayanti et al. (2010), reported clarification of tender coconut water using commercial UF, 50 kDa molecular weight cut off (MWCO), flat sheet membrane in a stirred cell. The specific flux was in the range of 16–20 l/m^2.h.bar. In this work, it was shown that polarization layer resistance, irreversible fouling resistance and membrane hydraulic resistance, all three are competitive and significant. However, sensory analysis and acceptability of the processed juice were not determined. Also, experiments were conducted in a stirred filtration cell and thus cannot be scaled up to an industrial level. In all the above works, experimental flux decline data are of little importance for process scaling up and they lack in detailed study of shelf life of the filtered juice.

In the present work, "cold sterilization" of tender coconut water was performed using highly scalable hollow fiber platform. A resistance-in-series model was formulated and used for analysing decline of permeate flux with operating conditions as well as identifying the limiting transmembrane pressure drop. All the quality parameters of the filtered juice were monitored after aseptic packaging. Since, thermal sterilization was not used, sensory properties of the product remained intact. Ultrafiltered juice was rich in polyphenol and potassium. The storage study was undertaken for eighteen weeks. Since, there are no additives or preservatives added externally and as the filtration is performed in a scalable system, the developed technology has immense potential for direct industrial scale application.

2. Theory

Flux decline during ultrafiltration of fruit juice is due to development of a fouling layer of rejected solutes on membrane surface (Mondal and De, 2010; Roy and De, 2014). Thus, the resistances encountered by the solvent during its permeation are membrane hydraulic resistance (R_M) and fouling resistance (R_F). For nascent membrane, R_M^0 is the membrane hydraulic resistance. After first run, the membrane resistance is determined from pure water run asR_M^1, where$R_M^1 = R_M^0 + R_{irr}^1$. R_{irr}^1 is the irreversible membrane resistance after washing at the end of first experiment. Therefore, the membrane resistance corresponding to the Nth experiment is directly measured as,

$$R_M^N = R_M^{N-1} + R_{irr}^N = \frac{\Delta P}{\mu_w \nu_w^0} \tag{1}$$

where, ΔP is the transmembrane pressure drop (TMP), μ_w is the viscosity of the water ($\mu_w = 0.9 \times 10^{-3}$ Pa s at 30 °C, measured using U-Tube viscometer) and ν_w^0 is the pure water flux at the end of Nth experiment (flux is the volume of filtrate per unit time, per unit area of the membrane) through the membrane. Thus, the irreversible membrane resistance is included in the estimation of membrane resistance corresponding to Nth experiment. The fouling layer resistance at any point of time can be determined from the experimental flux decline. It can be represented as,

$$R_F^N = \frac{\Delta P}{\mu(\nu_w(t))} - R_M^N \tag{2}$$

where, μ is the viscosity of the permeating solution ($\mu = 10^{-3}$ Pa s at 30 °C, measured using U-Tube viscometer) and $\nu_w(t)$ is the permeate flux through the membrane.

For a cross flow system, the growth of fouling resistance attains a steady state due to forced convection of retentate stream and the phenomenon is adequately described by a first order growth law (De et al., 1997),

$$\frac{dR_F^N}{dt} \alpha \left(R_F^{SN} - R_F^N\right) \tag{3}$$

where, R_F^{SN} is the steady state fouling resistance. The above expression can be integrated with an initial condition, at $t = 0, R_F^N = 0$.

$$R_F^N = R_F^{SN}[1 - \exp(-kt)] \tag{4}$$

where, k is the proportionality constant in Eq. (4). It may be noted that 'k' represents the rate of growth of the fouling layer. Therefore, a plot of $\ln\left[(R_F^{SN})/(R_F^{SN} - R_F^N)\right]$ with't' yields a straight line through origin with a slope 'k'.

3. Experimental

3.1. Materials

Tender coconut was purchased from local market in Indian Institute of Technology, Kharagpur, West Bengal, India. Polyacrylonitrile (PAN) co-polymer (copolymer of acrylonitrile, methyl acrylate, methacrylic acid in the ratio 96:3:1) of average molecular weight 150 kDa was purchased from M/s, Technorbital, Kanpur, India. N, N-dimethyl formamide (DMF), sodium hydroxide (NaOH) and polyethylene glycol (Molecular weight 200, 100, 35, 20, 10, 6, 4 and 0.4 kDa) were procured from M/s, Merck (India) Ltd. Storage bottles of glass were obtained from Borosil Glass Works Ltd. (India) and polypropylene bottles were purchased from Tarsons Products Pvt. Ltd. (India).

3.2. Membrane preparation

85 wt% of DMF was heated at 60 °C and 15 wt% PAN copolymer was added. The copolymer of PAN was used to achieve high flux membrane (Thakur and De, 2012). The solution was stirred using a REMI stirrer (supplied by M/s, Anupam Enterprise, Kharagpur, India) at 50 rpm for 6 h till a homogenous solution was formed. The solution was then cooled to room temperature. The polymer solution was transferred to the polymer tank in the spinning unit. Hollow fibers were extruded using the gas pressure in a nitrogen cylinder with bore fluid distilled water. The fibers were allowed to fall in the gelation bath containing tap water at room temperature completing the phase inversion process. The detailed spinning conditions are presented in Table 1. It has been well established in the literature that hydrolysis of PAN membrane reduces the MWCO of the membrane (Parashuram et al., 2013; Abedi et al., 2015). The effect of hydrolyzation time on the MWCO of the membrane is presented in Fig. S1 in the supplementary section. It can be clearly asserted that a MWCO of the 44 kDa can be achieved by subjecting the membrane to prolong contact with NaOH. Hence, the hollow fibers were then dipped in 1 (N) NaOH solution for 36 h and dried in

Table 1
Specification of hollow fiber spinning unit.

Inner diameter of the spinneret, m	0.0005
Outer diameter of the spinneret, m	0.012
Air gap between extrusion point and gelation bath, m	0.25
Casting temperature, K	300
Pressure in polymer-melt tank, kPa	35
Water flow rate, m^3/s	3.3×10^{-7}
Flow rate of polymer solution, kg/s	5×10^{-5}
Inner diameter of the hollow fiber, m	0.0006
Outer diameter of the hollow fiber, m	0.0008
Inner diameter of membrane module, m	0.0118
Length of membrane module, m	0.2
Number of hollow fibers packed in the module	70
Total membrane area, m^2	0.025

an oven at 40 °C. 70 hollow fibers were then potted in a PVC pipe to make the module. Details of spinning conditions, fiber and module specifications are presented in Table 1.

3.3. Experimental set up and procedure

Tender coconut water was first passed through a 150 μm nylon mesh to eliminate suspended debris and the feed was prepared. It was then subjected to cross flow ultrafiltration in the hollow fiber set up. The feed was pumped from a 3 l feed tank using a booster pump and was fed to the hollow fiber module. The retentate was recycled through a rotameter to the feed tank. TMP across the module was determined by taking the average of the pressure gauge reading at the inlet and outlet of the module. TMP and cross flow rate (CFR) were independently set using the pump bypass valve and the retentate valve. Experiments were conducted at eight TMP values, 21, 42, 63, 84, 103, 138, 172 and 193 kPa and CFRs were 5, 10 and 15 l/h (Reynolds number 51, 101 and 152, respectively). TMP and CFR were maintained independently and total 24 experiments were conducted. Duration of each experiment was 1 h. Details of the experimental set up are shown in Fig. 1(a). Fig. 1(b) represents the laboratory scale membrane module and set up.

Cumulative permeate was collected and the permeate flux was measured from the slope of cumulative volume versus time data. The permeate stream was analyzed in terms of pH, colour, clarity, conductivity, total soluble sugar, total protein, polyphenol, sodium and potassium.

Before starting of the UF experiments with the tender coconut water feed, the membranes were first compacted with distilled water at 193 kPa for 3 h. Then steady state permeate flux was noted at different TMPs. The membrane permeability was estimated from the slope of permeate flux versus TMP plot. After each run, the membrane was washed using tap water for 30 min followed by distilled water for 15 min to recover the membrane permeability as much as possible. All the experiments were conducted in triplets and the mean value and standard deviation (SD) is reported in the figures and tables.

3.4. Membrane characterization

3.4.1. Hydraulic permeability and molecular weight cut off (MWCO) of the membrane

The membrane hydraulic permeability was measured by plotting the pure water flux at different TMP. The slope of the straight line passing through origin gives the permeability of the membrane (L_P). The membrane hydraulic resistance (R_M^N) can be represented in terms of permeability as,

$$R_M^N = \frac{1}{\mu_w L_P} \tag{5}$$

where, μ_w is in Pa.s, L_P is in m/Pa.s and R_M^N is in m^{-1}

The MWCO of the membranes was calculated by measuring the rejection of polymeric solutes of different molecular weights (4 kDa, 6 kDa, 10 kDa, 20 kDa, 35 kDa, 70 kDa, 100 kDa and 200 kDa) as mentioned in section 3.1. A solution of 10 kg/m^3 was prepared by dissolving the polymers in distilled water and was fed to the feed chamber. The experiment was conducted at 70 kPa and at a cross flow rate of 10 l/h to minimize the concentration polarization effect. The permeate was collected at intervals of 5 min and the concentration was measured using a digital refractometer (supplied by M/s Cole-Palmer, Kolkata, India) and the percentage rejection (%R) was measured as,

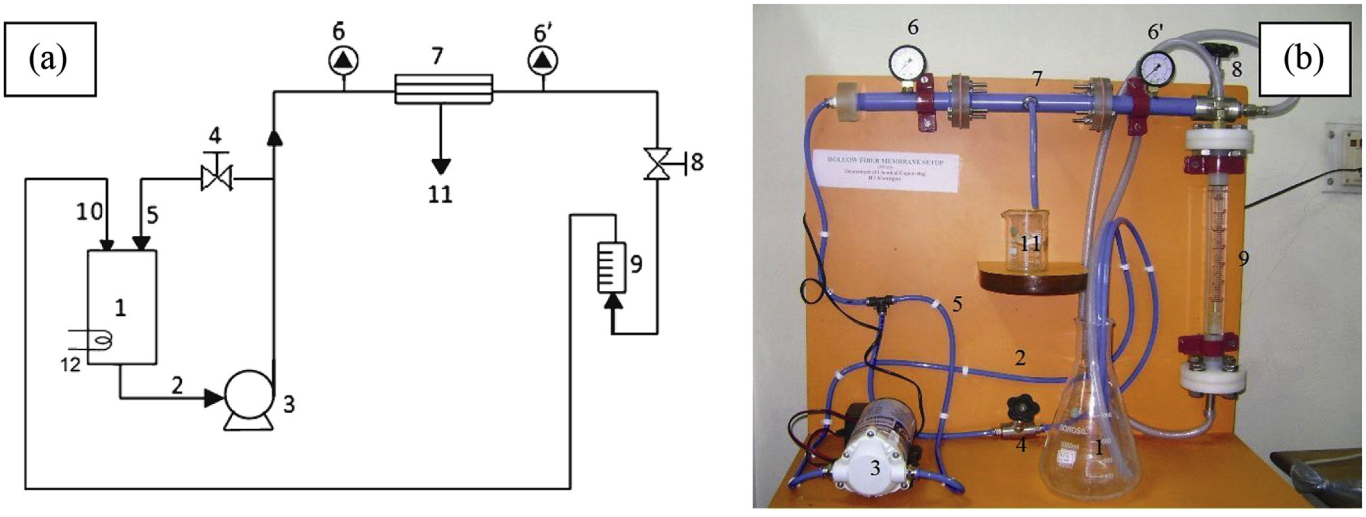

Fig. 1. (a) Schematic diagram of tangential ultrafiltration unit with recycle mode; (b) Laboratory scale setup. 1: Feed tank; 2: suction pipe; 3: feed pump; 4: bypass valve; 5: bypass pipe; 6 and 6': pressure gauge (at the inlet and outlet of the membrane module); 7: membrane module; 8: flow control valve; 9: rotameter; 10: flow pipe; 11: permeate; 12: heat exchanger.

$$\%R = \left(1 - \frac{C_P}{C_F}\right) \times 100\% \quad (6)$$

where, C_P is concentration of permeate and C_F is concentration of feed. The rejection (R) was calculated and plotted against the logarithm of the molecular weight of the solutes. The point where 90% rejection was obtained, the corresponding molecular weight gave the MWCO of the membrane (Panda and De, 2014). The average pore radius () of the membrane was calculated using Eq. (7) (Singh et al., 1998).

$$r_{avg} = 16.73 \times 10^{-10}(MWCO)^{0.557} \quad (7)$$

where, r_{avg} is the average pore radius in cm, MWCO is the molecular weight cut off in Dalton.

3.4.2. Surface morphology study

The surface morphology of the membranes was studied using Scanning Electron Microscope (SEM) images (model: ESM-5800, JEOL, Japan). The membranes were dried in dessicator overnight. The dried membranes were then dipped in liquid nitrogen for 5 min and fractured for the cross sections views.

3.5. Analysis

The permeate was analyzed for its clarity, total poly-phenols, protein concentration, colour, pH, total soluble sugar (TSS), sodium, potassium and conductivity for each stream (Sagu et al., 2014). Variation of colour and clarity was studied for the storage study.

Colour of the extract was measured by absorbance (A) at a wavelength of 420 nm using a spectrophotometer (M/s Perkin Elmer, Connecticut, USA) (Rai et al., 2010). Clarity of the extract was measured by transmittance (%T) at 660 nm using the same spectrophotometer (Rai et al., 2010).

Total poly-phenol was measured using a modified Folin and Ciocaltaeu method (Vasco et al., 2008). Briefly, 0.5 ml of the coconut water blank or standard was placed in a 25 ml flask and 0.5 ml of the Folin–Ciocaltaeu reagent was added. The mixture was allowed to react for 5 min with stirring. 10 ml of solution of sodium carbonate (concentration 75 g/l) was added and mixed well. The volume was then completed up to 25 ml with distilled water and kept at room temperature for 1 h. The absorbance was then measured at 750 nm using a spectrophotometer (M/s, Perkin Elmer, Connecticut, USA). The results were expressed as mg of Gallic acid equivalent per 100 ml (mg GAE/100 ml).

Particle size of the feed and clarified coconut water was measured by Zetasizer (model: Zetasizer nano ZS90) supplied by M/s, Malvern Instruments, Worcestershire, UK.

Protein concentration was determined according to the dye binding method of Lowry method (Lowry et al., 1951) with bovine serum albumin (BSA) as standard.

The total soluble solids content in degree Brix (°Brix) was determined using an ABBE type refractometer (Excel International, Kolkata, India).

Conductivity and pH values of juice were measured using a multi parameter pocket tester (EUTECH Instruments Ltd, Singapore). The unit for conductivity is μS/cm.

Concentration of potassium and sodium was determined using ion-selective electrode potentiometer (Thermo Scientific, Beverly, MA 01915 USA). The results are given in mg/l.

The analyses were repeated three times and the mean value and standard deviation (SD) is reported in the figures and tables.

3.6. Storage study and taste analysis

The storage study was carried out for filtered tender coconut water for 18 weeks using borosilicate glass bottle and polypropylene bottles. The experiments were conducted in a cross flow hollow fiber ultrafiltration module. The whole set up was enclosed in a laminar hood chamber to avoid any bacterial contamination during collection. All the pipe lines, pump and valves were washed with 30% H_2O_2 or ethyl alcohol and kept at 80 °C for 15 min to remove any bacteria present. The samples were collected in sample bottles. The bottles were washed with ethyl alcohol and kept in hot air oven for 15 min at 60 °C. They were filled to the brim during the collection without head space. After the collection, the bottles were wax sealed and kept at a refrigerated temperature of 5 °C.

The taste analysis was performed by a series of experts in a 9 point hedonic scale (Ranganna, 2005), where the rating varies from 1 (dislike extremely) to 9 (like extremely). Then rankings were given accordingly. The Fiducial limits for Hedonic rating were calculated and checked whether the hedonic mean score was above or below the fiducial limit. The taste analysis was undertaken for the sample that was kept in refrigerated condition for four weeks. The taste analysis was performed on the basis of appearance, texture, aroma, flavour, colour, overall quality and purchase intention.

4. Results and discussion

4.1. Membrane characterization

Hydraulic resistance of the nascent membrane was 2.5×10^{12} m^{-1}. MWCO of the membrane was determined from the curve of rejection of neutral solutes with their molecular weight as shown in Fig. 2 (a). MWCO of the membrane estimated from this figure was 44 kDa with average pore radius 6.5 nm, i.e., average pore diameter is 13 nm (from Eq. (7)). Scanning electron micrograph images of the cross section of the pristine hollow fiber and treated one (as discussed in section 3.2) are presented in Fig. 2 (b) and (c). It is observed that the hollow fiber has a thin dense skin followed by finger like pores spreading across the cross section. The magnified view of the hollow fibers near the inner wall is shown in Fig. 2(d) and (e). These figures clearly indicate the asymmetric structure of hollow fibers. Effects of alkali treatment followed by annealing are apparent from further magnified (20000× with a scale bar 1 μm) SEM views of the inner surface of both the hollow fibers as described in Fig. 2(f) and (g), respectively. It is observed from these figures that the inner skin is really dense with smaller pores which can be seen. From Fig. 2(g), it is evident that pore sizes in the skin layer of hollow fiber are reduced compared to that in the untreated hollow fiber, thereby creating a denser membrane. This observation is in line with the result shown in Fig. 2(a) that the treatment protocol described in section 3.2 results into converting the untreated membrane from microfiltration (Thakur and De, 2012) to ultrafiltration range (44 kDa).

4.2. Effects of operating condition

Particle size distribution of the feed and the permeate is shown in Fig. 3. It is observed that there are two distinct size distributions of the particles in the feed: (i) smaller range from 0.4 to 6 nm and (ii) higher range from 300 to 600 nm. The average membrane pore radius is 6.5 nm, as discussed earlier. Thus, smaller sized fraction of the particles in the feed are easily permeated through the membrane and the larger sized fraction causes a deposition of particles on membrane surface causing the growth of the fouling layer. The

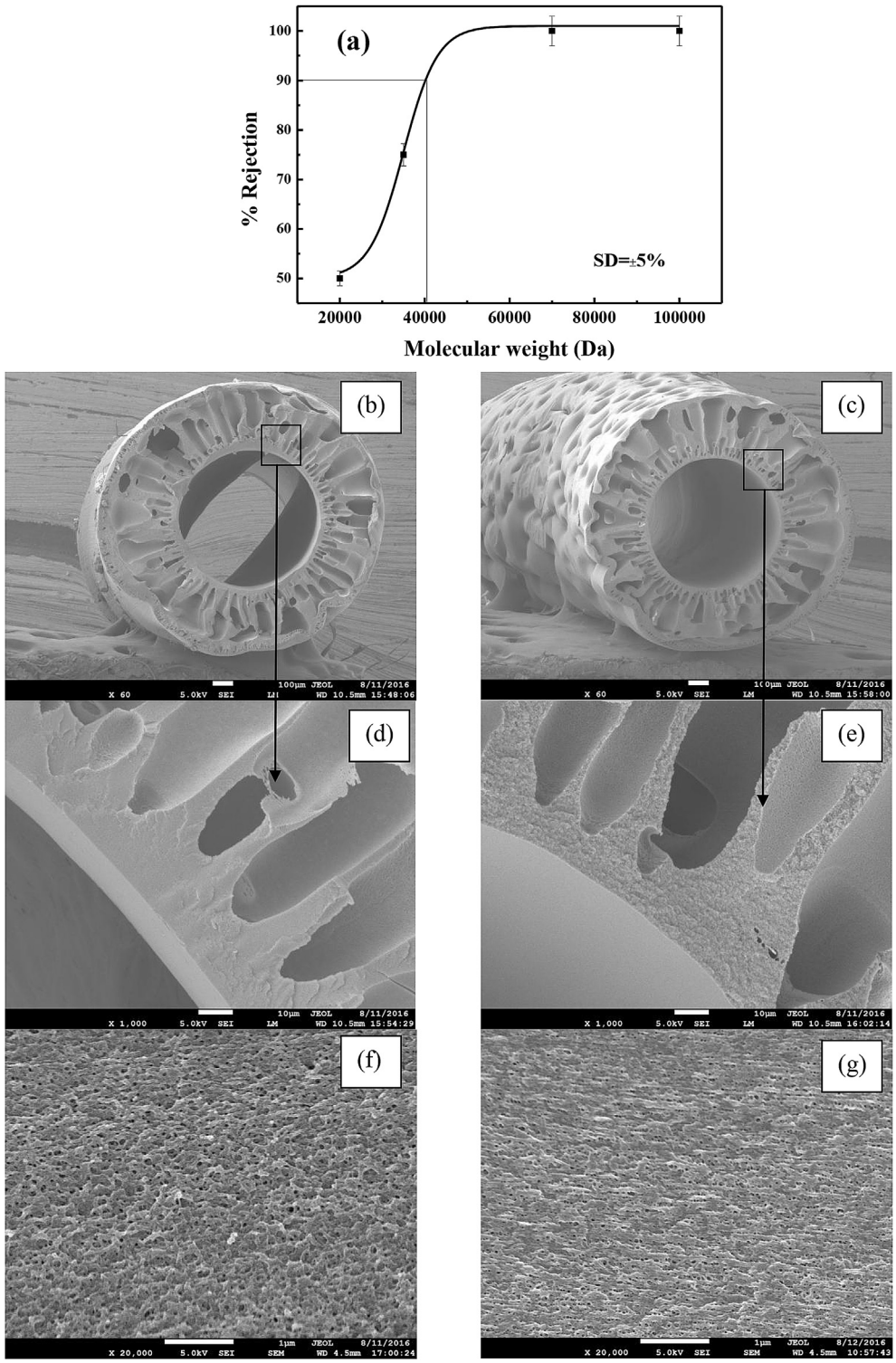

Fig. 2. (a) MWCO of the hydrolyzed PAN membrane and SEM images of (b) cross section of copolymeric PAN membrane; (c) cross section of hydrolyzed PAN membrane; (d) skin layer of copolymeric PAN membrane; (e) skin layer of hydrolyzed PAN membrane; (f) inner surface of copolymeric PAN membrane and (g) inner surface of hydrolyzed PAN membrane.

flux decline profiles for various operating conditions are presented in Fig. 4 and Fig. S2 in supplementary section. It is observed from Fig. 4 (a) to 4 (c), that the steady state is achieved within first 30 min for all the operating conditions. TMP has more pronounced effect on the flux profile than Reynolds number. The extent of membrane fouling (extent of flux decline) during an experiment is evident from this figure for different operating conditions. The flux decline is minimum for the highest Reynolds number at a particular TMP.

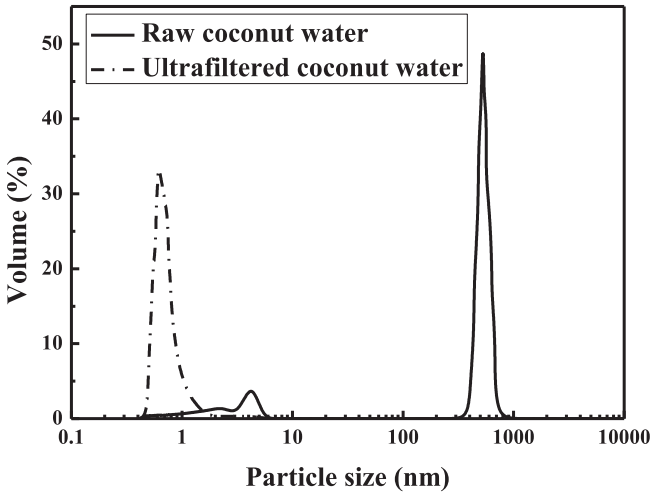

Fig. 3. Particle size distribution for raw coconut water and ultrafiltered coconut water.

Higher Reynolds number imparts more shear on the fouling layer over the membrane surface leading to lowering in resistance against the solvent transport, thereby improving the permeate flux. For example, at 21 kPa TMP and Re = 152, the flux decline is 34% (from 25 l/m^2.h to 16.6 l/m^2.h). The corresponding value of flux decline at Re = 52 is 36%. Therefore, in the selected range of Reynolds number, this effect on flux decline is insignificant. However, as mentioned earlier, TMP has a remarkable effect of flux decline behaviour. For example, at 21 kPa and Re = 152, the flux decline is 34%. At the same Reynolds number, this value is 60% for 138 kPa and 72% for 193 kPa. More solutes are convected towards the membrane surface at higher TMP, leading to higher fouling resistance resulting in higher flux decline.

4.3. Membrane hydraulic resistance and cleaning efficiency

The permeability after each run was measured and the membrane hydraulic resistance (R_M^N) was determined using Eq. (5). As evident from this figure, the membrane hydraulic resistance varies in the range of 2.86×10^{12} m^{-1} to 4×10^{12} m^{-1}. The variation of membrane hydraulic resistance with the number of experiments (N) is shown in Fig. 5. The hydraulic resistance can be correlated to the number of runs using the following equation,

$$R_M^N = 4 \times 10^{12} - 1.4 \times 10^{12} \exp\left(-N/5\right) \quad (8)$$

where, R_M^N is in m^{-1}. The correlation coefficient of the above fit is 0.98. It is observed that some amount of membrane permeability is lost permanently due to incomplete cleaning of the membrane. Irreversible membrane resistance corresponding to each experiment is evaluated according to Eq. (1) and presented in Fig. S3 in supplementary section. It is clear from this figure that the irreversible resistance is upto 9% of the membrane hydraulic resistance. Thus, variation of irreversible resistance is insignificant compared to membrane resistance.

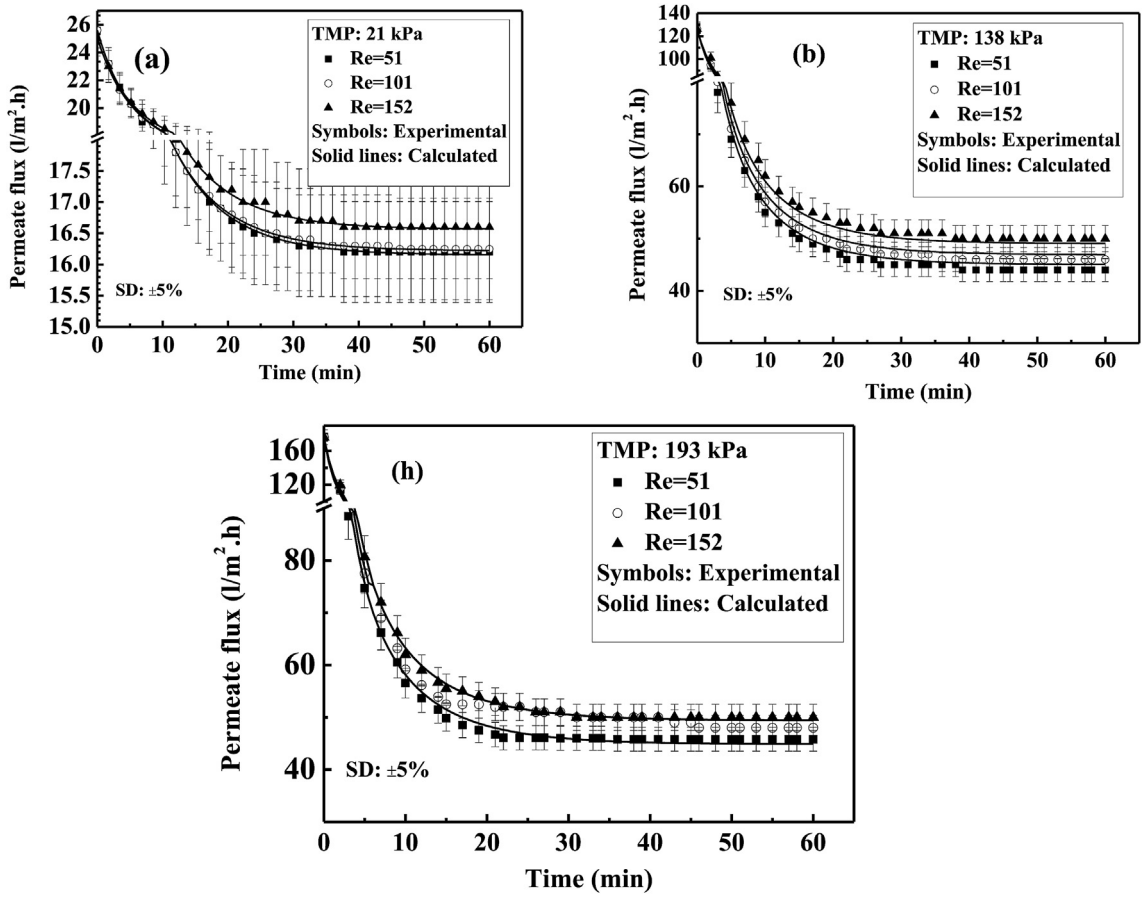

Fig. 4. Calculated and experimental flux profiles at various TMP and Re. (a) 21 kPa; (b) 138 kPa and (c) 193 kPa.

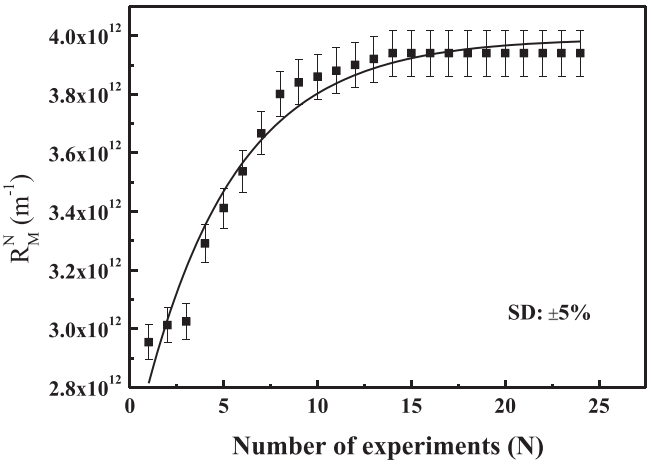

Fig. 5. Variation of membrane hydraulic resistance with number of experiments.

4.4. Determination of fouling resistance (R_F^N)

The fouling resistance for the Nth run was determined using Eq. (2). The other parameters R_F^{SN} and k represent the steady state fouling resistance and the rate constant for the growth of the fouling layer, respectively. The steady state fouling resistance for all the operating conditions is correlated with TMP and Re as,

$$\frac{R_F^{SN}}{R_M^N} = \left(0.5 - 6.1 \times 10^{-4} Re\right) \exp\left(9.6 \times 10^{-3} \Delta P\right) \quad (9)$$

where, ΔP is in kPa and R_M^N is in m^{-1}.

Correlation coefficient of the above equation is 0.99 and hence, it adequately captures the effect of operating conditions onR_F^{SN}. As evident from the equation, with increase in TMP, the fouling resistance also increases and it decreases with Reynolds number. This can be attributed to the fact that at higher TMP more solutes are convected towards the membrane surface leading to higher fouling resistance. Conversely, at higher Reynolds number the thickness of the fouling layer decreases due to enhanced turbulence.

The rate of growth of fouling resistance was estimated from the slope of straight line fit of $\ln\left[(R_F^{SN})/(R_F^{SN} - R_F^N)\right]$ with time't'. This was carried out for all operating conditions. A typical plot at TMP 172 kPa and Re = 152 is shown in Fig. 6. The value of k for this operating condition is 0.0021 s^{-1}. Similar analysis was carried out for all the operating conditions and it was found that k varied in a narrow range between 0.0019 s^{-1} and 0.0022 s^{-1}. An average value of k = 0.002 s^{-1} is, therefore, used for all the operating conditions.

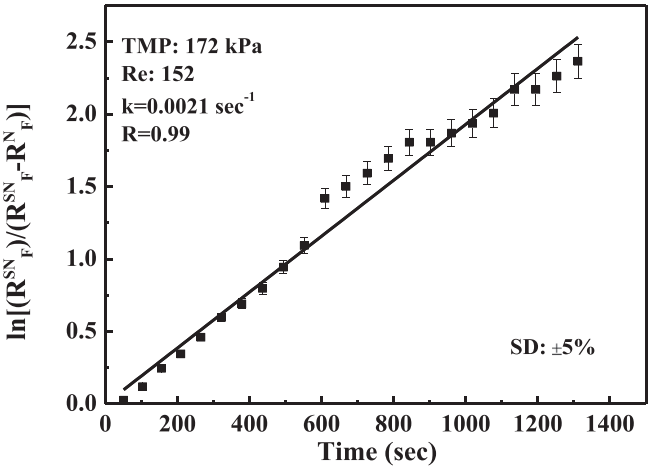

Fig. 6. Estimation of k values at TMP 172 kPa at Re = 152.

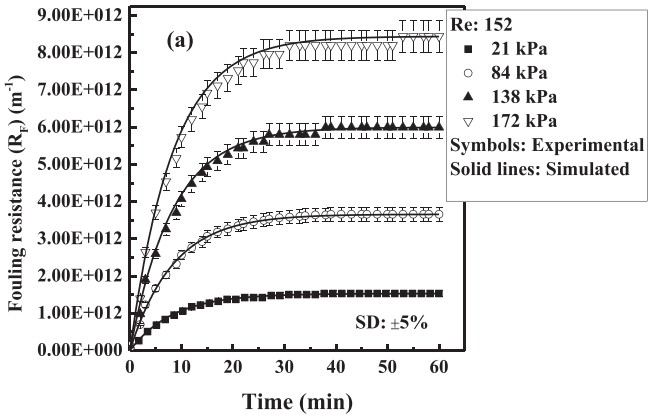

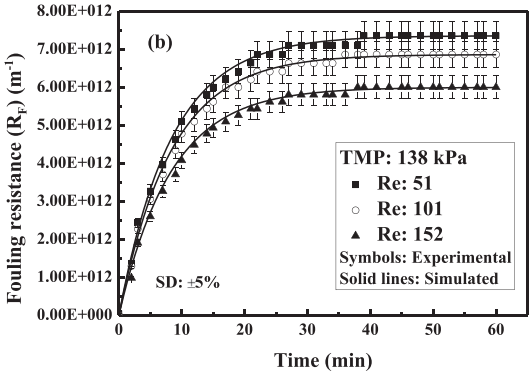

Fig. 7. Comparison between the experimental and calculated fouling resistance for (a) different TMP at Re = 152 and (b) at different Reynolds number at TMP = 138 kPa.

The experimental and calculated values of fouling resistance at 21, 84, 138 and 172 kPa are shown in Fig. 7(a) at Reynolds number 152. As evident from this figure, the calculated fouling resistance nearly corroborates with the experimental data, suggesting good fit at different TMPs and the range of Reynolds number studied herein.

4.5. Estimation of correlation of permeate flux

The experimental and correlated permeate flux plot is shown in Fig. 4 and Fig. S2 (in supporting document), where, the solid lines represent the calculated flux and the symbols represent the experimental flux values. The flux profile at any time period for the Nth experiment can be represented using the following equations,

$$v_w(t) = \frac{3.6 \times 10^6 \Delta P}{\mu\{4 \times 10^{12} - 1.4 \times 10^{12} \exp(-N/5)\}\left[\begin{array}{l} 1 + (0.5 - 6.1 \times 10^{-4} Re)\exp(9.6 \times 10^{-3} \Delta P) \\ \times\{1 - \exp(-2 \times 10^{-3} t)\}\end{array}\right]} \quad (11)$$

$$v_w(t) = \frac{\Delta P}{\mu\left[R_M^N + R_F^N\right]} \quad (10)$$

Combining Eqs. (4) (8) (9) and (10), the expression of permeate flux becomes,

where, ΔP is in kPa, μ is in Pa.s, v_w is in l/m^2.h. As evident from Fig. 4 and Fig. S2 (in supporting document), the experimental values are close to the calculated flux values, suggesting that the proposed model adequately captures the filtration behaviour. Variation of experimental steady state flux with various TMP at different Reynolds number is plotted in Fig. 8(a). At the steady state, $1 - \exp(-2 \times 10^{-3} t) \approx 1$ in Eq. (11) and the corresponding permeate flux can be estimated as a function of TMP and Reynolds number. It is clear from Fig. 8(a) that the calculated flux values agree clearly with the experimental data. Effect of TMP is more pronounced than Re number on steady state flux. For example, at Re = 152, the steady state flux increases from 16.6 l/m^2.h to 50 l/m^2.h (more than 3 times increment) as TMP increases from 21 to 193 kPa. This trend is expected due to increase in the driving force. On the other hand, increase in Reynolds number prevents the undisturbed growth of fouling resistance, leading to flux enhancement. However, it may be observed that the enhancement of permeate flux due to Reynolds number is not very significant in the range studied herein. At 21 kPa, steady state flux increases from 16.2 to 16.6 l/m^2.h (only 4% increase) with the increase in Reynolds number from 51 to 152 and at higher TMP, i.e., 193 kPa the steady state flux increases from 46 l/m^2.h to 50 l/m^2.h (only 8% increase). Another phenomenon that can be observed is that, at higher pressure range, i.e., 172 and 193 kPa, the steady state flux remains almost invariant. It is in the range of 46–50 l/m^2.h with varying Reynolds number (flux decline data for TMP, 42, 63, 84, 103 and 172 kPa are shown in the supporting Fig. S2). This occurrence can be attributed to the fact that at such TMP, the limiting flux was attained. Hence, it can be asserted that any TMP beyond this range will not enhance the productivity of the membrane. The limiting flux or the pressure independent flux can be determined by computing $dv_w^s/d\Delta P$ to zero and the resultant relationship between limiting TMP and Re is obtained as,

$$\left[9.6 \times 10^{-3} \Delta P_{lim} - 1\right]\exp\left(9.6 \times 10^{-3} \Delta P_{lim}\right) = \frac{1}{0.5 - 6.1 \times 10^{-4} Re} \quad (12)$$

where, ΔP_{lim} is in kPa. This equation presents the locus of TMP and Re at limiting conditions and this curve is presented by the solid line in Fig. 8 (b). It is clear from this figure that steady state permeate flux under limiting conditions increases with Reynolds number. At a higher Re, higher TMP is required to attain the limiting flux. For example, limiting TMP increases from 153 kPa to 160 kPa as Reynolds number varies from 50 to 200. This indicates that enhanced shearing effect by forced convection imposed by the retentate flow rate extends the onset of the limiting conditions. In this context, limiting TMP can be compared with threshold TMP that is defined as the maximum TMP till the flux-TMP relationship is linear (Bachhin et al., 2006; Field and Pearce, 2011; Roy and De, 2014). Threshold pressure for various operating conditions is evaluated from Fig. 8(a) and presented in Fig. 8(b). It is evident from this figure that threshold pressure also increases with Reynolds number and at higher Re, it approaches the limiting pressure. However, realization of sufficient high Reynolds number is limited by the pump capacity and geometrical configuration of the membrane module.

4.6. Quality of permeate

The analysis of the permeate samples with respect to the feed are presented in Table 2. It is observed from Table 2, that for most of the operating conditions, sodium, potassium, polyphenol and total

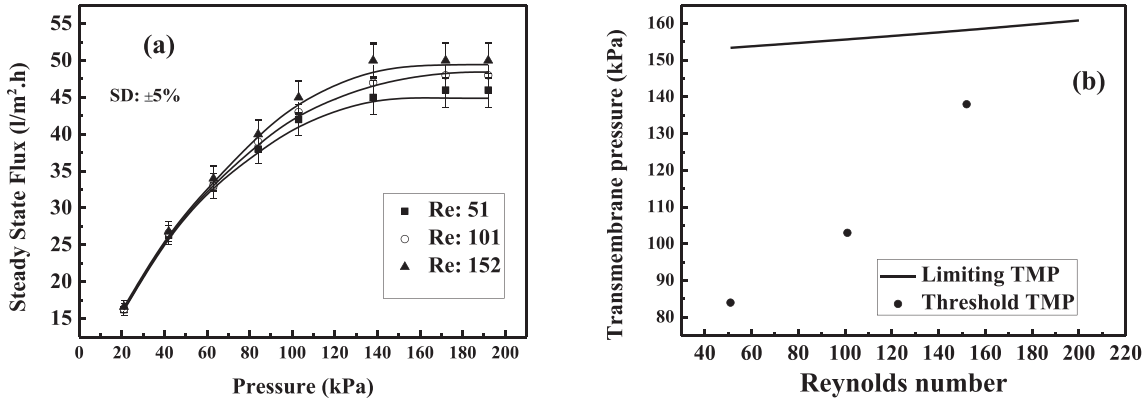

Fig. 8. (a) Variation of steady state permeate flux with TMP and Re; (b) Limiting and threshold TMP as function of Reynolds number.

Table 2
Properties of feed and permeate samples at different operating conditions.

Number of experiments	Pressure drop (kPa)	Flow rate (l/h)	pH	Conductivity (mS/cm)	Clarity (%T)	TSS (°Brix)	Total solid (% wt)	Sodium (mg/l)	Potassium (mg/l)	Total protein (mg/l)	Polyphenol (mg/l)
Feed	–	–	5.4 ± 0.3	6.2 ± 0.2	89.94 ± 0.5	6.1 ± 0.5	7.0 ± 0.5	50 ± 2	4012 ± 118	4993 ± 120	20 ± 1.5
1	21	5	5.3 ± 0.2	5.2 ± 0.1	98.9 ± 0.4	3.0 ± 0.3	2.7 ± 0.2	15 ± 1.5	1419 ± 65	3170 ± 98	16 ± 1
2	21	10	5.3 ± 0.4	4.2 ± 0.2	98.8 ± 0.2	2.9 ± 0.4	2.8 ± 0.3	18 ± 1.2	1519 ± 70	2675 ± 102	16 ± 1.2
3	21	15	5.2 ± 0.2	4.3 ± 0.3	99.1 ± 0.4	2.9 ± 0.4	2.8 ± 0.1	20 ± 1.5	1708 ± 52	2685 ± 104	15 ± 1.1
4	42	5	5.4 ± 0.1	4.3 ± 0.2	99.2 ± 0.5	2.6 ± 0.3	2.1 ± 0.2	21 ± 2	2197 ± 64	2780 ± 85	15 ± 0.8
5	42	10	5.1 ± 0.3	4.3 ± 0.2	99.1 ± 0.3	2.8 ± 0.4	2.0 ± 0.2	25 ± 0.9	2277 ± 54	1922 ± 89	16 ± 0.9
6	42	15	5.2 ± 0.4	5.6 ± 0.1	98.9 ± 0.5	2.9 ± 0.2	2.1 ± 0.2	25 ± 1.2	2401 ± 60	1707 ± 78	15 ± 1.1
7	63	5	5.3 ± 0.2	4.3 ± 0.2	99.2 ± 0.2	3.2 ± 0.3	2.2 ± 0.3	26 ± 1.3	2510 ± 75	1878 ± 101	15 ± 1.2
8	63	10	5.2 ± 0.3	5.2 ± 0.1	99.4 ± 0.3	3.4 ± 0.4	2.5 ± 0.2	28 ± 1.8	3050 ± 98	1926 ± 98	16 ± 0.9
9	63	15	5.4 ± 0.4	5.7 ± 0.2	99.4 ± 0.2	3.5 ± 0.2	2.8 ± 0.1	30 ± 1.2	3275 ± 112	1622 ± 112	15 ± 1.1
10	84	5	5.1 ± 0.3	5.8 ± 0.2	99.1 ± 0.3	3.1 ± 0.3	2.5 ± 0.2	31 ± 1.4	3300 ± 105	1560 ± 95	15 ± 1.1
11	84	10	5.6 ± 0.2	5.6 ± 0.3	99.2 ± 0.2	3.2 ± 0.2	2.6 ± 0.3	30 ± 1.3	3295 ± 80	1520 ± 95	14 ± 1.3
12	84	15	5.2 ± 0.3	4.9 ± 0.4	99.3 ± 0.3	3.1 ± 0.3	2.9 ± 0.1	29 ± 1.2	3315 ± 85	1425 ± 97	15 ± 1.4
13	103	5	5.4 ± 0.1	5.1 ± 0.3	99.1 ± 0.5	3.2 ± 0.3	2.8 ± 0.2	31 ± 1.8	3165 ± 75	1385 ± 101	16 ± 0.9
14	103	10	5.3 ± 0.2	5.6 ± 0.3	99.2 ± 0.6	3.1 ± 0.3	2.5 ± 0.2	32 ± 1.2	3230 ± 95	1415 ± 85	17 ± 0.8
15	103	15	5.1 ± 0.3	5.2 ± 0.2	99.4 ± 0.2	3.1 ± 0.2	2.3 ± 0.2	33 ± 1.3	3320 ± 90	1478 ± 97	16 ± 1.2
16	138	5	5.4 ± 0.1	5.2 ± 0.3	99.6 ± 0.1	3.3 ± 0.3	2.4 ± 0.3	31 ± 1.5	3510 ± 80	1350 ± 97	16 ± 1.3
17	138	10	5.5 ± 0.2	4.8 ± 0.4	99.2 ± 0.2	3.2 ± 0.1	2.6 ± 0.2	30 ± 1.9	3125 ± 70	1450 ± 85	15 ± 0.7
18	138	15	5.6 ± 0.3	5.1 ± 0.2	99.1 ± 0.6	3.4 ± 0.3	2.9 ± 0.1	31 ± 1.6	3213 ± 85	1510 ± 94	16 ± 1.2
19	172	5	5.4 ± 0.2	5.1 ± 0.3	99.7 ± 0.4	3.1 ± 0.2	2.8 ± 0.2	30 ± 1.7	3150 ± 75	1490 ± 89	17 ± 0.8
20	172	10	5.8 ± 0.4	4.3 ± 0.1	98.8 ± 0.6	3.2 ± 0.3	2.6 ± 0.3	29 ± 1.3	3219 ± 85	1525 ± 82	15 ± 1.5
21	172	15	5.2 ± 0.1	4.8 ± 0.2	99.1 ± 0.2	2.9 ± 0.1	2.7 ± 0.1	31 ± 1.9	3275 ± 70	1475 ± 94	16 ± 0.8
22	193	5	5.1 ± 0.4	4.7 ± 0.3	99.2 ± 0.3	2.8 ± 0.2	2.3 ± 0.2	31 ± 1.8	3190 ± 75	1385 ± 95	16 ± 0.9
23	193	10	5.2 ± 0.3	4.7 ± 0.4	99 ± 0.3	3.1 ± 0.3	2.6 ± 0.2	30 ± 1.3	3275 ± 105	1427 ± 99	15 ± 1.2
24	193	15	5.6 ± 0.2	4.9 ± 0.2	98.8 ± 0.4	3.0 ± 0.1	2.8 ± 0.2	32 ± 1.5	3402 ± 101	1498 ± 88	16 ± 1.1

The analyses were conducted in triplets, the mean value and the standard deviations are reported.

soluble solids (TSS) (the nutritional qualities) in the feed have been partially permeated in the filtrate. As evident from the physico-chemical analysis of the permeate obtained at different operating conditions, the variation is insignificant with respect to TMP and Re. Hence, the optimum values of the operating condition are determined at 138 kPa and 15 l/h which yields the highest productivity (50 l/m^2.h). At this condition, about 56% of TSS, 60% of sodium, 80% of potassium and polyphenol have been permeated in the filtrate. During filtration, higher molecular weight solutes like, protein, polysaccharides, etc., form a fouling layer over the membrane surface that acts as a dynamic membrane retaining partially the lower molecular weight aforementioned nutritional components.

4.7. Storage study

As discussed earlier, the storage study was carried out for filtered tender coconut water for 18 weeks using borosilicate glass bottle and poly-propylene bottles. Various parameters of the extract, namely, TSS, pH, sodium, potassium, clarity, polyphenol, protein content and total solids were monitored with interval of one week. The results are presented in Fig. 9 and Fig. S4 (in supporting document). It is observed from these figures that variation of the quality parameters is marginal for both the bottles. This indicates that both types of bottles are suitable for storing the treated coconut water. Except protein (Fig. 9) and total solids (Fig. S4), all other parameters decrease. The extent of decrease for various nutritional parameters over 19 weeks is, TSS: 14%; sodium: 20%; potassium: 25%; polyphenol: 68% and pH 23%. The undesirable qualities, protein and total solids increase over 19 weeks by 50% and 56%, respectively. Thus, increase in total solids concentration is mainly due to increase in proteins. Interestingly, the protein concentration increases by only 23% for 18 weeks and after that it increases significantly. It can also be observed that clarity of stored juice over 19 weeks is reduced by only 5% and the taste is intact within 18 weeks (as described in the following section). Therefore, the extract can be stored successfully for 18 weeks.

4.8. Taste analysis

For taste, the fiducial limit was calculated in a 9 point Hedonic scale. A series of unbiased experts had tasted the juice after each month of storage study. The rating was done based on appearance, texture, aroma, flavour, colour, overall quality. The Fiducial limits for Hedonic rating were calculated as 0.7 to 1.8 at 1% and 0.9 to 1.6 at 5% probability level for a control sample. All the mean values for appearance, texture, aroma, flavour, colour and overall quality on a hedonic scale were below the fiducial limit. Hence, the ultrafiltration permeate was absolutely fine after 18 weeks of storage. All the persons taking part in the rating process confirmed positive purchase intention. The mean score of the samples were 0.5, 1.0, 0.6, 0.5 and 0.8, respectively. The taste was acceptable even after 18 weeks of storage.

5. Conclusion

- 44 kDa, PAN hollow fiber membrane treated with sodium hydroxide was used for clarification of tender coconut water.
- The throughput of PAN membrane was 50 l/m^2.h at the optimum operating condition of 138 kPa transmembrane pressure and 15 l/h cross flow rate.
- The resistance-in-series model was adequate to explain the flux behaviour of the filtration system.
- The limiting TMP as obtained from the modelling were in the range of 153–158 kPa for Reynolds number 51 to 152. Hence, the optimum operating TMP was selected at 138 kPa.
- The storage study was conducted for 18 weeks and it was observed that all the physico chemical properties, especially nutritional qualities like sodium, potassium, TSS and polyphenol showed marginal deviation from the initial value. Thus, the sample did not deteriorate after 18 weeks of storage in aseptic packaging in both borosilicate and poly-propylene bottles.
- It was confirmed by a series of experts that the taste was good and all showed positive purchase intention till 18 weeks.

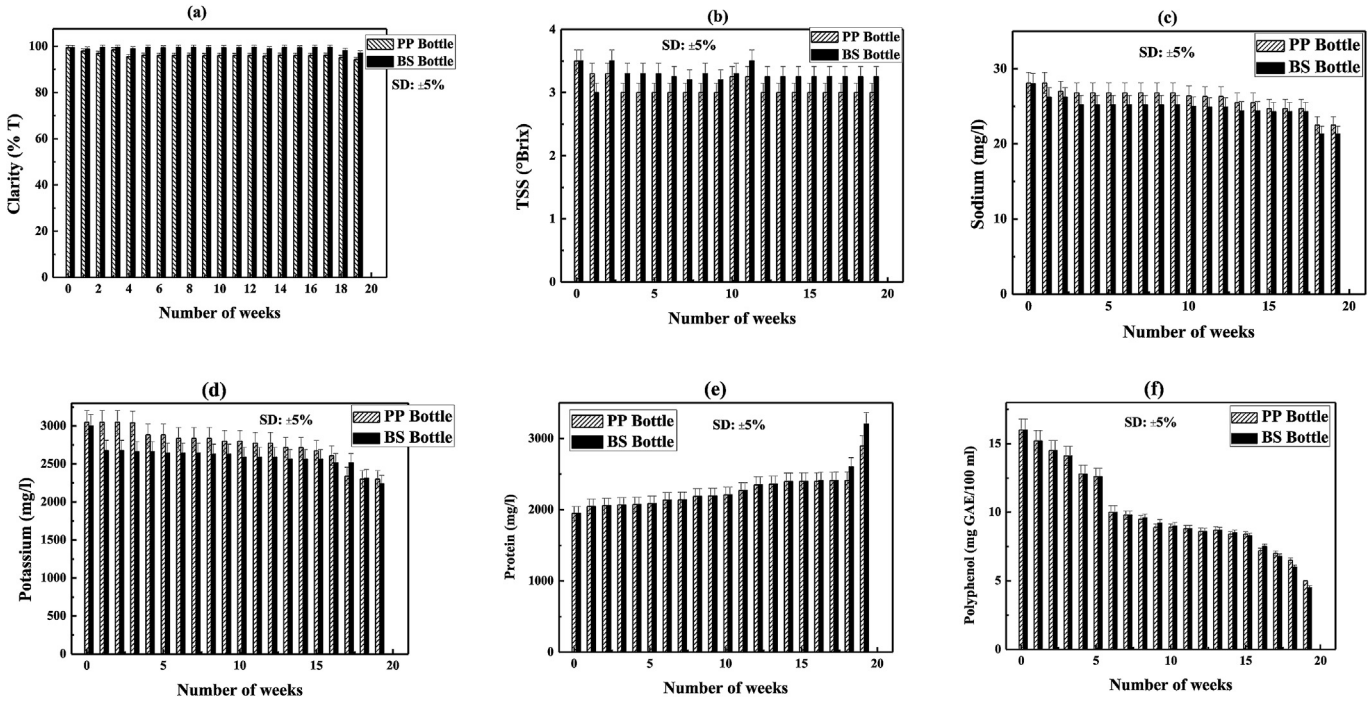

Fig. 9. Storage study results for 18 weeks for (a) clarity, (b) TSS, concentration of (c) sodium, (d) potassium, (e) protein and (f) polyphenol at refrigerated temperature (5 °C).

Conflict of interest

The authors declare no competing financial interest.

Acknowledgement

This work is partially supported by Technoeagles Pvt. Ltd., Pune, INDIA, a grant from the SRIC, IIT Kharagpur under the scheme no. IIT/SRIC/CHE/SMU/2014-15/40, dated 17-04-2014 and funding from INAE Chair Professorship of Prof. S. De. The authors would also like to thank Mr. Mrinmoy Mondal for his valuable inputs and help in this work. Any opinions, findings and conclusions expressed in this paper are those of the authors.

Appendix A. Supplementary data

Supplementary data related to this article can be found at http://dx.doi.org/10.1016/j.jfoodeng.2016.12.021.

Nomenclature

C_F	Concentration of feed (kg/m^3)
C_P	Concentration of permeate (kg/m^3)
k	Rate of growth of the fouling layer (s^{-1})
L_P	Membrane permeability (m/Pa.s)
N	Number of experiments
r_{avg}	Average pore size (m)
%R	Rejection (%)
Re	Reynolds number
R_F	Fouling resistance (m^{-1})
R_F^N	Fouling resistance for the Nth run (m^{-1})
R_F^{SN}	Steady state fouling resistance for the Nth run (m^{-1})
R_{irr}	Irreversible membrane resistance (m^{-1})
R_{irr}^N	Irreversible membrane resistance for the Nth run (m^{-1})
R_M^0	Membrane hydraulic resistance for nascent membrane (m^{-1})
R_M^N	Membrane hydraulic resistance for the Nth run (m^{-1})
t	Time (s)
v_w^0	Pure water flux (l/m^2.h)
v_w^s	Steady state permeate flux (l/m^2.h)
v_w	Permeate flux (l/m^2.h)

Greek symbols

ΔP	Transmembrane pressure (kPa)
ΔP_{lim}	Limiting transmembrane pressure (kPa)
μ	Viscosity of the permeating solution (Pa.s)
μ_w	Viscosity of water (Pa.s)

References

Abedi, M., Sadeghi, M., Chenar, M.P., 2015. Improving antifouling performance of PAN hollow fiber membrane using surface modification method. J. Taiwan Inst. Chem. Eng. 55, 42–48.
Bachhin, P., Aimar, P., Field, R.W., 2006. Critical and sustainable fluxes: theory, experiments, and applications. J. Membr. Sci. 281, 48–69.
Campos, C.F., Souza, P.E.A., Coelho, J.V., Gloria, M.B.A., 1996. Chemical composition, enzyme activity and effect of enzyme inactivation on flavor quality of green coconut water. J. Food Process. Preserv. 20, 487–500.
De, S., Dias, J.M., Bhattacharya, P.K., 1997. Short and long term flux decline analysis in ultrafiltration. Chem. Eng. Commun. 159, 67–89.
Field, R.W., Pearce, G.K., 2011. Critical, sustainable and threshold fluxes for membrane filtration with water industry applications. Adv. Colloid Interface Sci. 164, 38–44.
Jayanti, V.K., Rai, P., Dasgupta, S., De, S., 2010. Quantification of flux decline and design of ultrafiltration system for clarification of tender coconut water. J. Food Process Eng. 33, 128–143.
Jackson, J.C., Gordon, A., Wizzard, G., McCook, K., Rolle, R., 2004. Changes in chemical composition of coconut (*Cocos nucifera*) water during maturation of the fruit. J. Sci. Food Agric. 84, 1049–1052.
Lowry, O.H., Rosebroughi, N.J., Farr, A.L., Randall, R.J., 1951. Protein measurement with the folin phenol reagent. J. Biol. Chem. 193, 265–275.
Maciel, M.I., Oliviera, S.L., Da Silva, I.P., 1992. Effects of differentstorage conditions on preservation of coconuts (*Cocos nucifera*) water. J. Food Process. Preserv. 16, 13–22.
Magalhaes, M.P., Gomes, F.S., Modesta, R.C.D., Matta, V.M., Cabral, L.M.C., 2005. Conservation of green coconut water by membrane filtration. Cienc. Tecnol.

Aliment. 25, 72–77.
Magda, R., 1992. Coco soft drink: health beverage from coconut water. Food Mark. Technol. 6, 22–23.
Matsui, K.N., Granado, L.M., de Oliveira, P.V., Tadini, C.C., 2007. Peroxidase and polyphenol oxidase thermal inactivation by microwaves in green coconut water simulated solutions. LWT- Food Sci. Technol. 40, 852–859.
Matsui, K.N., Gut, J.A.W., de Oliveira, P.V., Tadini, C.C., 2008. Inactivation kinetics of polyphenol oxidase and peroxidise in green coconut water by microwave processing. J. Food Eng. 88, 169–176.
Mondal, S., De, S., 2010. A fouling model for steady state crossflow membrane filtration considering sequential intermediate pore blocking and cake formation. Sep. Purif. Technol. 75, 222–228.
Panda, S.R., De, S., 2014. Preparation, characterization and performance of $ZnCl_2$ incorporated polysulfone (PSF)/polyethylene glycol (PEG) blend low pressure nanofiltration membranes. Desalination 347, 52–65.
Parashuram, K., Maurya, S.K., Rana, H.H., Singh, P.S., Ray, P., Reddy, A.V.R., 2013. Tailoring the molecular weight cut off values of polyacrylonitrile based hollow fibre ultrafiltration membranes with improved fouling resistance by chemical modification. J. Membr. Sci. 425–426, 251–261.
Rai, C., Rai, P., Majumdar, G.C., De, S., Dasgupta, S., 2010. Mechanism of permeate flux decline during microfiltrationof watermelon (*Citrullus lanatus*) juice. Food Bioprocess Technol. 3, 545–553.
Ranganna, S., 2005. Handbook of Analysis and Quality Control for Fruit and Vegetable Products, fourth ed. Tata Mcgraw Hill, New Delhi, India.
Reddy, K.V., Das, M., Das, S.K., 2005. Filtration resistances in nonthermal sterilization of green coconut water. J. Food Eng. 69, 381–385.
Reddy, K.V., Das, M., Das, S.K., 2007. Nonthermal sterilization of green coconut water for packaging. J. Food Qual. 30, 466–480.
Roy, A., De, S., 2014. Resistance-in-series model for flux decline and optimal conditions of Stevia extract during ultrafiltration using novel CAP-PAN blend membranes. Food Bioprod. Process. 94, 489–499.
Saat, M., Singh, R., Sirisinghe, R.G., Nawawi, M., 2002. Rehydration after exercise with fresh young coconut water, carbohydrate-electrolyte beverage and plain water. J. Physiol. Anthropol. Appl. Hum. Sci. 21 (2), 93–104.
Sagu, S.T., Karmakar, S., Nso, E.J., Kapseu, C., De, S., 2014. Ultrafiltration of banana (*Musa acuminata*) juice using hollow fibers for enhanced shelf life. Food Bioprocess Technol. 7, 2711–2722.
Singh, S., Khulbe, K.C., Matsuura, T., Ramamurthy, P., 1998. Membrane characterization by solute transport and atomic force microscopy. J. Membr. Sci. 142 (1), 111–127.
Thakur, B.K., De, S., 2012. A novel method for spinning hollow fiber membrane and its application for treatment of turbid water. Sep. Purif. Technol. 93, 67–74.
Vasco, C., Ruales, J., Kamal-Eldin, A., 2008. Total phenolic compounds and antioxidant capacities of major fruits from Ecuador. Food Chem. 111, 816–823.
Yong, J.W.H., Ge, L., Ng, Y.F., Tan, S.N., 2009. The chemical composition and biological properties of coconut (*Cocos nucifera* L.) water. Molecules 14, 5144–5164.